

Review

# Current Transition of Nucleation and Growth under Diffusion-Controlled ElectrocrySTALLIZATION: A Brief Review

Gong Luo <sup>1,2</sup> , Yuan Yuan <sup>1,2,\*</sup>, De-Yu Li <sup>2</sup>, Ning Li <sup>2</sup> and Guo-Hui Yuan <sup>2</sup>

<sup>1</sup> Guangdong Provincial Key Laboratory of Petrochemical Equipment and Fault Diagnosis, College of Mechanical and Electrical Engineering, Guangdong University of Petrochemical Technology, Maoming 525000, China

<sup>2</sup> School of Chemistry and Chemical Engineering, Harbin Institute of Technology, Harbin 150001, China

\* Correspondence: yyuan865@hit.edu.cn

**Abstract:** A brief review is given on the current transition of the electrodeposition of materials by a mechanism of nucleation followed by diffusion-controlled growth. A short historical background to study the nucleation and growth by diffusion-controlled electrocrysTALLIZATION is provided. Then, an outline of the major potentiostatic current transient modeling is given, with some comments on their relative merits. Finally, a summary of the current transition functions of nucleation and growth under diffusion-controlled electrocrysTALLIZATION is given including the theoretical models that have been recently applied.

**Keywords:** current transition; nucleation and growth; diffusion-controlled; electrocrysTALLIZATION



**Citation:** Luo, G.; Yuan, Y.; Li, D.-Y.; Li, N.; Yuan, G.-H. Current Transition of Nucleation and Growth under Diffusion-Controlled ElectrocrySTALLIZATION: A Brief Review. *Coatings* **2022**, *12*, 1195. <https://doi.org/10.3390/coatings12081195>

Academic Editor: Alina Pruna

Received: 10 June 2022

Accepted: 15 August 2022

Published: 16 August 2022

**Publisher's Note:** MDPI stays neutral with regard to jurisdictional claims in published maps and institutional affiliations.



**Copyright:** © 2022 by the authors. Licensee MDPI, Basel, Switzerland. This article is an open access article distributed under the terms and conditions of the Creative Commons Attribution (CC BY) license (<https://creativecommons.org/licenses/by/4.0/>).

## 1. Introduction

One of the first topics within the context of electrochemistry is electrochemical metal deposition. With applications in domains such as electrodeposition and solution analysis, electrochemical deposition is a topic of great interest from both a theoretical and practical standpoint. As reviews in 'Electrochimica Acta' in 2000 [1] and 'Journal of Electroanalytical Chemistry' in 2003 [2] indicate, considerable work has been conducted on investigating the mechanism of such deposition over the last 70 years [3]. Metal electrodeposition occurs at electrode/electrolyte interfaces under the influence of an electric field and includes a number of phase formations. The initial stages in the electrochemical phase formation processes strongly depend on nucleation and growth. Through the study of electrocrysTALLIZATION, Milchev et al. elaborated the thermodynamics and kinetics related to the electrochemical nucleation and growth of nanoclusters on solid surfaces and integrated the corresponding theoretical and experimental phenomena [4]. The crystal growth during electrodeposition directly determines the structure of deposits. The physical, chemical, electric, and magnetic characteristics of metal deposits such as metal films, modulated multilayers and sandwich structures, and low-dimensional metal systems are determined by nucleation-and-growth processes in electrochemical metal deposition. Future nanotechnology will heavily rely on electrochemically generated nanostructures, particularly for the creation of nanoelectronic devices such as quantum dots and single-electron devices as well as the creation of novel materials with unconventional properties [1]. The atomic structure of the deposit and the surface inhomogeneities of the substrate have a significant impact on the early phases of nucleation and growth processes. Native substrates do not require nucleation, and the growth method is influenced by the substrate's perfection and the overpotential or supersaturation. The most crucial factors in the overall deposition mechanism on foreign substrates are the metal–substrate interaction, the crystallographic metal–substrate misfit, the overpotential, and the deposition rate. Nucleation is necessary for the majority of electrocrysTALLIZATION processes.

Through nucleation and growth, electrodeposition takes place. Electrocrysallization is a typical nucleation and growth process in electrochemical metal deposition that has long attracted the interest of scientists and engineers [5–9]. According to the nucleation-rate rule, nuclei form at active sites on the substrate and expand as more ions from the solution are incorporated. The study of nucleation by electrochemical techniques has several benefits over other ways of investigating heterogeneous nucleation because electrocrysallization and electrochemical reaction occur at the same time. An important aspect of the study of the electrocrysallization mechanism is to establish the functional relationship between the metal-ion reduction current and microcrysallization kinetic process parameters, and to use the current function of electrocrysallization to study the microcrysallization kinetic process. Thus, the microcrysallization-and-growth process of a coating was analyzed, and the crystal-structure information of the electrodeposited coating was obtained including metal ion-mass transfer, electrodeposited crystal-nucleus density, coating grain size, and so on. However, considerable controversy remains over even the most basic principles involved in modeling and the current-time-functions of such systems, as discussed in recent studies [8,10–14].

This brief review tries to evaluate the state of affairs in one specific field of electrodeposition: deposition with diffusion-controlled growth, with a focus on the extraction of current-time functions. Three aspects of this were considered: the diffusion-controlled electrocrysallization process, theoretical modeling, and current transition function.

## 2. Diffusion-Controlled Electrocrysallization Process

Electrodeposition is a complicated electrochemical process. Positive ions near the cathode obtain electrons and are reduced to metal atoms. Individual metal atoms adsorb onto one another to form metal nuclei and grow gradually. Finally, they can become visible metal deposits, which is called metal electrocrysallization. Electrocrysallization is a complicated multistep chain reaction involving the diffusion and mass transfer of ions in solution, the removal of solvation shells, electron transfer, the formation of surface adsorbed atoms, the clustering of adsorbed atoms, the generation of crystal nucleus, or embedding into existing lattice. The study of the dynamic process of electrocrysallization has always been an important content of electrocrysallization theory and has attracted considerable attention in the field of electrochemistry. The nucleation-and-growth process is the most important research content and has been widely researched [8,9].

In the early stage, electrodeposition theory focused on the crystal-growth interface structure of electrocrysallization and its effect on the formation of new phases on the electrode surface. Stranski [15] studied the difference of nucleation energy at different sites at the solid-liquid interface, indicating that the new phase was more easily generated at steps or terraces of multiple contact surfaces. According to the theory of electrodeposition microgrowth and the crystallization process, the electrodeposition process can be described as shown in Figure 1.

With further research development, considering that electrocrysallization occurs at the solid-liquid interface, the electrochemical nucleation process inevitably produces partially charged particles (i.e., a partially hydrated molecule). Conway et al. [16] calculated that the charge transfer was more likely to occur in the plane position of the electrode surface. The preferential growth of the lattice at the step or corner was proposed to be accompanied by the surface diffusion of adsorbed particles. Subsequently, Vermilyea and Fleischmann et al. [17,18] introduced the spiral-dislocation crystal-growth theory into the electrocrysallization theory to explain the spiral-dislocation growth observed on the electrodeposited copper surface [19,20].

Electrocrysallization is a multistep chain process whose reaction completion is controlled by the slowest step. Accordingly, researchers have studied rate-controlling steps to reflect the entire electrocrysallization process. Theoretically, any step of electrocrysallization can become a rate-controlling step. In fact, nucleation and growth can be broadly classified into two categories: ‘interfacial (or charge) controlled’, in which the nucleus-

growth rate is limited by the rapidity with which ions can be incorporated into the new phase, and ‘diffusion controlled’, in which nucleus growth is limited by the rate at which a material is transported through the solution onto the electrode surface. Certain systems also tend toward one or the other due to their complex mechanisms. However, most electrochemical crystallization processes are performed under diffusion control. Furthermore, in the electroplating process controlled by diffusion mass transfer, most metal-electroplating processes are performed by 3D nucleation growth, except for a few metals that show single-layer deposition or two-dimensional nucleation growth such as silver electrodeposition [21–23]. This field has also received the greatest concern in the study of the electocrystallization mechanism, and it is also the main aspect to be summarized in the next section of this paper.

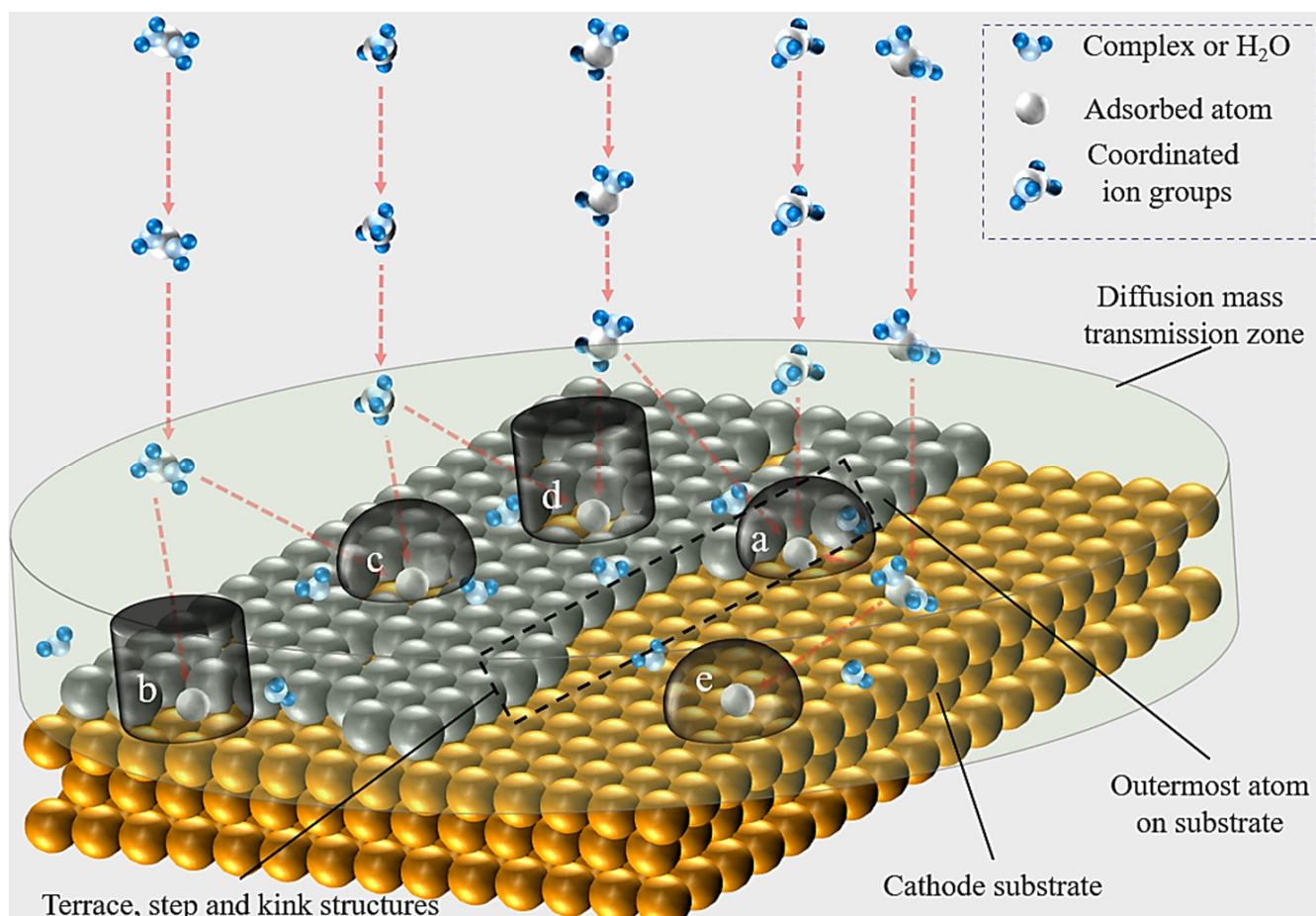


**Figure 1.** A schematic of the electocrystallization process. (a,c) Hemispherical diffusion zone on the terrace, step, and kink sites. (b,d) Cylindrical diffusion zone on the terrace, step, and kink sites. (e) Cylindrical or hemispherical diffusion zone on the plane surface. The red dashed arrows represent the ion transport path.

The establishment and research of diffusion-controlled potentiostatic current transient modeling is based on spherical nucleation and growth. The general idea of establishing the model in the study was based on the mass-transfer process of a single-nucleus point. The calculation of current-time transformation on an electrode surface is also based on the current transformation of single-nucleus electrodeposition, which is then extended to the process of multinucleus interaction superposition. The establishment of the coating nucleation-and-growth model controlled by diffusion and mass transfer is usually described as follows. Nuclei are generally accepted to have a hemispherical shape. The radius ' $r'$  of a hemispherical nucleus that grows under pure diffusion control is obtained by combining Faraday's law with the time-independent part of the hemispherical diffusion equation. In other words, the nucleus has such a small size that it can be considered

as an ultramicroelectrode. As the radii of the diffusion zones grow and overlap, the electrodeposition current decreases quickly. Many researchers have applied Avrami's theorem to describe how diffusion zones grow and overlap on the electrode surface.

Next, this paper summarizes the research on the establishment of a diffusion-controlled 3D nucleation-and-growth model and the calculation of the current transformation. Other nucleation-and-growth processes are not specifically summarized and discussed.

### 3. Model of Nucleation and Growth

Armstrong et al. [24] studied the nucleation-and-growth process of electrocrystallization. They proposed the formation and growth of 3D conical nuclei during electrocrystallization in 1966 and discussed the current transformation process of the electrocrystallization. Subsequently, Bosco et al. [25,26] theoretically studied the electrocrystallization process of nuclei with different shapes and found that the theoretical current of hemispherical 3D nucleus growth showed the characteristics of changing from maximum to minimum before reaching the final current, which was the closest to the actual electrocrystallization current transformation process.

The potentiostatic current–time transition curve of electrodeposition nucleation growth is the most extensively used research method of electrodeposition nucleation. As early as 1958, researchers [27] used the ‘constant voltage’ method, in which the constant potential after the potential step is applied to the battery and the current generated as a function of time is measured as a method of extracting information about nucleation. Then, Astley et al. [28] simulated the movement of hemispherical nuclei with radius ‘ $R$ ’ and volume ‘ $V$ ’ in a solution of ions with the deposition concentration ‘ $c$ ’ and considered the diffusion coefficient ‘ $D$ ’ of fast and slow ion migration in the electrolyte. The flux of ionic charge per unit time on the hemispherical surface will be equal to the current during electrodeposition. Researchers have also studied the relationship between flux to the nuclei and the process of crystallization [29]. Next, the crystal growth model and current transition function of the 3D nucleation process of electrocrystallization with diffusion-controlled ion migration and mass transfer as the control step are summarized.

In the 1980s, Scharifker et al. [29–32] systematically discussed the microdynamic process of electrocrystallization based on the study of 3D spherical nucleus-growth model and infinite diffusion mass-transfer theory, the so-called SH model. The SH model is based on the variation law of a single-core time current, superimposes the current of each core point according to the random distribution law of nuclei points, describes the relationship between core points with Avrami's theorem [33–36], and finally calculates the expression of time–current [30]. The relationship between  $I_{(1,t)}$  and time  $t$  is described in Equation (1).

$$I_{(1,t)} = zF\pi (2Dc)^{3/2} M^{1/2} t^{1/2} / \rho^{1/2} \quad (1)$$

The nomenclature used for the variables, parameters, and constants are explained at the end of the manuscript. In the case of the random distribution of multiple-discharge nuclei on the electrode surface, Avrami's theorem is used to describe the interaction between the nuclei and the diffusion-influence region in the SH model, which has a time-dependent diffusion-influence region radius. Finally, the current density-transition functions of multi-nucleus point-discharge deposition can be obtained as follows:

Instantaneous nucleation is described by Equation (2):

$$I = zFcD^{1/2} / (\pi t)^{1/2} (1 - \exp(-N\pi kDt)) \quad (2)$$

Progressive nucleation is described by Equation (3):

$$I = zFcD^{1/2} / (\pi t)^{1/2} \left( 1 - \exp \left( -AN_m \pi k'Dt^2 / 2 \right) \right) \quad (3)$$

To simply describe the time–current transformation of the coating nucleation-and-growth process, the SH theoretical model converts the time–current relationship into a

dimensionless one, its current density is transformed into  $\left(\frac{I}{I_m}\right)^2$ , and time is transformed into  $(t/t_m)$ . The mathematical relationship after the dimensionless transformation is expressed as follows:

Instantaneous nucleation is described by Equation (4):

$$\left(\frac{I}{I_m}\right)^2 = \frac{1.9542}{t/t_m} \{1 - \exp [-1.2564(t/t_m)]\}^2 \quad (4)$$

Progressive nucleation is described by Equation (5):

$$\left(\frac{I}{I_m}\right)^2 = \frac{1.2254}{t/t_m} \{1 - \exp [-2.3367(t/t_m)^2]\}^2 \quad (5)$$

These current–time-functions establish a clear bridge between the macrotransient current and the microprocess of electrocrystallization, thereby providing a method of electrochemical *in situ* analysis of the electrocrystallization mechanism. The expression after dimensionless transformation is simple and convenient in practical application, and is extensively used in electrodeposition research. These functional relations are also well-verified by experiments on the transient–current curve measured with a glassy carbon electrode. Therefore, the SH model is the first theoretical study in the literature to complete the establishment of the nucleation-and-growth model of electrocrystallization under complete diffusion control and the calculation of the current–transition function formula, which is extensively recognized and applied in electroplating research such as Au [37–40], Cu [41], Sn–Co [42], etc. However, in the long-term research process, some experimental tests of the nucleation process have revealed a certain deviation between the experimental test curve and the theoretical one described by the SH model [43–45]. In most reports in the literature, the experimental and theoretical curves of the SH model well agreed before the time corresponding to the current peak, but they showed deviations after the time corresponding to the current peak. The study also found that with prolonged time, the deviation between the experimental curve and the theoretical curve gradually expands. The difference in the current attenuation between the theoretical model current function and the experimental transient–current curve has gradually been put forward in a large number of studies. In other words, the attenuation speed of the actual current curve is slower than that of the SH model current–function curve, as reported in [43] (Figure 4), [44] (Figure 3), [45] (Figure 4) and [46] (Figure 7).

In light of this deviation, Scharifker et al. [44] proposed that the extra electrochemical reaction, excited by the change in the electrode-surface polarization state such as hydrogen evolution, compensates for the attenuation of the actual electrocrystallization current, so the attenuation of the actual current is slower than that of the theoretical current. This viewpoint provides a better explanation than the SH model for the electrocrystallization process containing hydrogen evolution. This extra reaction leads to the electrode test current being slightly higher than the current value described in the theoretical model for a long time. This view has a certain ability to explain the deviation of the curve measured at a relatively negative potential. However, the deviation between the experimental curve and the theoretical curve of some simple single-metal salts at a relatively low polarization is difficult to explain. Other researchers in the literature have primarily studied and discussed the distribution of core points on the electrode surface and the existence of multiple pairs of electrochemical reactions on the electrode surface [47–49].

Other researchers have attempted to improve the SH model from the aspects of electrocrystallization theory and kinetic mechanism. Mostany et al. [29] investigated the distribution of active points on the electrode surface and nucleation density and added the correction parameter ‘ $\alpha$ ’ into the SH model. The number of active points of electrocrystallization is introduced into the current function, and ‘ $\alpha$ ’ modifies the SH model by

adjusting itself to improve the matching degree between the original expression and the experimental curve.

In light of the difficulty of the SH model in describing electrodeposition under the condition of a large core density at the negative electrode potential, Heerman et al. discussed the situation of a high-density of active points and introduced the variables related to Dawson's integral ' $\Phi$ ' to modify the expression of the SH model [50]. Altimari et al. [51] proposed a mixed kinetic-diffusion control deposition model, discussed the distribution-and-growth process of crystal nuclei, and provided an explanation for the problem of current attenuation to zero.

The above discussions were based on the modification of SH model expression based on hemispherical infinite-diffusion process. Through some correction methods, the corresponding relationship between the experimental curves and the modified theoretical model was improved. However, through careful analysis of the functions established by the SH model, we found that the dimensionless Equations (4) and (5) could also be confirmed (i.e., when the independent variable of the expression increases, the value of its dependent variable continues to decay). When the electrocrystallization time reaches 100 times of  $t_m$  (the time value corresponding to the peak value of current density) in Equations (1) and (2), the current value decays to 1–2% of the peak current. This phenomenon obviously differs as the deposition current tends to be stable during actual electrodeposition.

Careful observation of the actual transient current curve revealed that when the time exceeded the time corresponding to the current peak, the electrodeposition current continued to decline with prolonged time, and its declining trend had a limit. Generally, during actual electrodeposition, the reaction on the electrode surface gradually stabilizes after the change in the electrode-surface state from a few seconds to tens of seconds at constant potential. The current at the electrode surface also showed a stable result. This phenomenon is essentially different from the continuous decline in current in the SH theoretical function in a long-time range, showing the inevitability of the SH theoretical curve's deviation from the experimental data in a long-time range.

In their work with current attenuation as the main research content, in 1999, D'Ajello et al. [43,52,53] discussed the electrodeposition nucleation model from the perspective of ion transport in the electrolyte and introduced the idea of a limited-diffusion region. In the microdynamic process of electrocrystallization, the Brownian motion region of ions was introduced. A migration boundary was considered to exist in the migration process of ions that is not controlled by the electric field. According to this idea, the parameters of the relationship formula of the electrocrystallization current function were calculated. The 3D instantaneous nucleation-growth process and 3D continuous nucleation-growth functions are described as follows.

Instantaneous nucleation is described by Equation (6):

$$j = 2\pi NDRzFc_0 b \left( 1 + \frac{RN^{1/2}}{\sqrt{at}} \right) [1 - \exp(-at)] \quad (6)$$

Progressive nucleation is described by Equation (7):

$$j = 2\pi N_\infty DRzFc_0 b \left( 1 + \frac{\sqrt{2} R \sqrt{AN_\infty}}{\sqrt{a't}} \right) [1 - \exp(-a't^2)] \quad (7)$$

Introducing parameter ' $R$ ' can solve the problem of the transient-current attenuation to zero. The model provides different explanations for the transient-current model of electrocrystallization from the perspective of ion migration. The current-transformation formula established by using ' $R$ ' can inhibit the current attenuation for a long time, primarily because of the existence of the  $\frac{RN^{1/2}}{\sqrt{at}}$  and  $\frac{\sqrt{2} R \sqrt{AN_\infty}}{\sqrt{a't}}$  terms in Equations (6) and (7).

Taking the studies of D'Ajello and Scharifker into consideration, Luo et al. [14] proposed that the key factor causing the deviation between the SH model and experimental

results was the stabilization and limitation of a diffusion mass-transfer region based on the study of the electroplating of gold and its alloys in 2018. The parameter 'R' (diffusion depth) was introduced, and a finite diffusion coating growth-and-nucleation model based on diffusion migration and mass-transfer depth extension with stability tendency was proposed. When the diffusion depth extended to infinity (i.e., 'R' is infinite), the expression of Equations (8) and (9) can be unified with Equations (2) and (3) in the SH model. Moreover, the random distribution and the overlapping diffusion regions on the surface of the multiple-discharge deposited nucleus points ( $N$ ) are still described by Avrami's theorem. The current-density transition process of the multinucleus point-discharge deposition process is obtained as follows.

Instantaneous nucleation is described by Equation (8):

$$I = zFc_0D^{1/2}/\pi^{1/2} \left( \frac{\sqrt{\pi D}}{R} + \frac{1}{\sqrt{t}} \right) (1 - \exp(-N\pi kDt)) \quad (8)$$

Progressive nucleation is described by Equation (9):

$$I = zFc_0D^{1/2}/\pi^{1/2} \left( \frac{\sqrt{\pi D}}{R} + \frac{1}{\sqrt{t}} \right) \times (1 - \exp(-AN_m\pi k'Dt^2/2)) \quad (9)$$

A comparison of the mathematical relations of Equations (2) and (3) with Equations (8) and (9) revealed that the diffusion depth in the model is described by the parameter 'R', and the attenuation of the theoretical current-transient function can be adjusted. Therefore, the unity of the model and the SH model is ensured. The SH model is a limiting case of this model (i.e., when ' $R \rightarrow \infty$ ', Equations (8) and (9) and the current-density Equations (2) and (3) in the SH model have the same mathematical expression). They also extended the current transient to the potential transient [13].

Hyde et al. [54] further considered that the SH model was limited to static analysis and proposed a transient model of the deposition current and electrodeposition model under the condition of forced convection. They demonstrated that a system involving multiple diffusion-controlled nucleation under hydrodynamic conditions can be effectively parameterized and used to extract the values of  $N_0$  and  $A$ . Then, the electrodeposition model under forced convection was established using a propeller to guide the solution through the electrode surface and wall-tube electrode. The applicability of the model to the nucleation and growth of lead under two sets of hydrodynamic conditions was studied and compared.

Stephens et al. [55] studied the nucleation and growth process using introduced auxiliary additives during the electrodeposition process. The mathematical model was compared with the experimental data. The simulation used estimates of the reaction-rate constants associated with an additive system comprising sodium sulfate electrolytes containing accelerator and inhibitor species. Based on the synergistic effect of various additive species, a validation of models for metal nucleation and growth processes was developed as computations were integrated with experiments. However, due to the complicated nature of the additive chemistry for the system studied there, additional refinement of the hypothesis is needed through further comparison with experiments in the future.

Branco's explanation of potentiostatic current transients during nucleation and diffusion-controlled growth took into account the contact angle between developing clusters and the electrode surface [56]. It was demonstrated that the contact angle had no impact on the non-dimensional plots of the currents normalized with respect to their maxima or the nucleation rates determined from the analysis of experimental transients. Their findings showed that taking contact angles other than  $90^\circ$  into account when analyzing experimental current transients usually results in a decreased number in the densities of active sites for nucleation. Taking the influence of contact angle between the spherical cap and the

electrode surface into consideration was the strength, but this work did not reveal the quantitative relationship between the contact angle and the description of potentiostatic current transients during nucleation and diffusion-controlled growth.

In diffusion-controlled 3D nucleation and growth, Mazaira [57] established an overlapping layered model in which the early formed diffusion region was larger than the later formed diffusion region, considering the difference of all diffusion regions in height. The layered overlapping model of the diffusion zone provided an improved description of compound nucleation growth with diffusion-controlled 3D growth. The model described the nucleation-and-growth process by the layered-stacking method but did not provide the exact current-transformation formula.

Mamme [58] believed that it is essential to consider both kinetic and mixed control regimes when interpreting electrochemical nucleation and growth processes. To describe the growth of an isolated nucleus, they solved a time-dependent multi-ion transport and reaction model using the finite element approach. They discovered that a nucleus that is lower than a certain size always begins to develop under kinetic control, even after the introduction of a suitably significant overpotential. This finding means that a transition occurs from kinetic to mixed and to diffusion control. The corresponding transition periods between growth regimes were identified, and it was discovered that they were inversely correlated with the abundance of active species, decreased exponentially with overpotential, and increased linearly with initial nucleus size. Both effects were more pronounced as the process transitions from kinetic to mixed-control.

According to Guo and Searson [59–61], an island-growth mechanism often drives the electrochemical deposition of a metal onto a foreign substrate. The onset potential for deposition shifting away from the metal–ion couple's equilibrium potential to the negative is a crucial aspect of island formation. They discussed how nucleation overpotential affects the kinetics of island growth, the effects of nucleation overpotential on island shape and orientation, and the effects of coupling between the island density (applied potential) and island size at coalescence (grain size). The dynamics of island formation were then proposed in terms of the contributions to vertical and lateral growth. The growth kinetics and properties of the islands were strongly influenced by nucleation potential, according to the results. Ion transport in the solution regulates the deposition process when the overpotential for nucleation is high. The dynamics of island growth can define the geometry of the island in systems with low nucleation overpotential. They also suggested a fresh Monte Carlo model.

Given the lack of understanding of the early stages of electrochemical nucleus formation, Ustarroz et al. [49] studied the early stages of silver nucleus electrodeposition on carbon substrates using aberration-corrected TEM with carbon-coated TEM grids as electrochemical electrodes. With the help of electrochemical measurements and access to as-deposited nucleus size distribution and structural description, they made significant progress toward understanding the mechanisms underlying nucleus electrodeposition. The findings indicate that the surface mobility and aggregation of nanoclusters dominate early nucleus formation. They came to the conclusion that electrochemical nucleation-and-growth models need to be updated and that the early stages of nucleus electrodeposition should take into account an electrochemical aggregative growth process. Then, they calculated the Volmer–Weber 3D island-nucleation mechanism that occurs during the initial stages of metal plating and film formation on low-energy substrates. The sizes of these crystal clusters are determined by the electrode-deposition material and are unrelated to the potential or deposition time. The equilibrium between the nucleation and surface diffusion of nanoclusters determines the shape of deposits [62].

Velmurugan [63] believed that three-dimensional nucleation and growth on active surface sites were the basic and important initial stages of metal electrodeposition. Nucleation/growth kinetics of individual silver crystals on the Pt surface were measured in this study. A series of parameters such as the number of active sites, kinetic time lag, and number of growing nuclei were obtained from the  $i-t$  curves.

Gliozzi et al. [48] proposed an ohmic model to represent the process of nucleation and growth of electrodeposited materials. They assumed that the ions used for electrodeposition were uniformly distributed in the electrolytic cell and that ionic currents were generated due to the bulk electric field. Taking the neutralization of metal ions at the electrode into consideration, the nucleation during electrodeposition was described by the kinetic equation. The characteristic time describing ion neutralization was negligible relative to the ion flight time across the cell. The analysis of the interaction between the bulk electric field and the applied electric field provided an analytical formula for the surface density of deposited ions and the current in the applied circuit. The influence of electric field in the substrate on the surface deposition was also considered in their work.

During the development of current transition models for the multiple nucleation and diffusion-controlled growth of electrodeposited materials, there are two main schools of thought. The first consideration is based on the modification of SH model expression based on the hemispherical infinite-diffusion process due to the SH model having a satisfactory performance for most potentiostatic testing. The second school recommends an independent method based on the perspective of ion transport in the electrolyte, for example, the assumption of a Brownian motion region of diffusion throughout the deposition process.

Any model's ability to accurately simulate a real electrodeposition process determines its utility in nature. A direct observation of the multiple nucleation and growth processes occurring at the electrode surface using modern characterization technology can provide a better understanding of the nucleation and growth process during electrodeposition.

#### 4. Summary of Current Transition of Nucleation and Growth

The description of the potentiostatic current transients during nucleation and diffusion-controlled growth reported are summarized in Table 1.

**Table 1.** A summary of the current-transition functions of nucleation and growth in the references.

Ref.	Theoretical Model	Current Transition Function Groups of Nucleation and Growth
1983/B. Scharifker and G. Hills [30]	Hemispherical infinite diffusion mass transfer model	<p>Group (1)</p> <p>For instantaneous nucleation:  <math>I = zFcD^{\frac{1}{2}}/(\pi t)^{\frac{1}{2}}(1 - \exp(-N\pi kDt));</math></p> <p>For progressive nucleation:  <math>I = zFcD^{\frac{1}{2}}/(\pi t)^{\frac{1}{2}}(1 - \exp(-AN_m\pi KDt^2/2))</math></p>
1984/B. Scharifker and J. Mostany [29]	Hemispherical infinite diffusion mass transfer model	<p>Group (2)</p> <p>Current transition function:  <math>I = \left(\frac{zFD^{\frac{1}{2}}c}{\pi^{\frac{1}{2}}t^{\frac{1}{2}}}\right)(1 - \exp\left\{-N_0\pi kD\left[t - \frac{1-e^{-At}}{A}\right]\right\})</math></p> <p>For instantaneous nucleation:  <math>\alpha \rightarrow 0: I = \left(\frac{a}{t^{\frac{1}{2}}}\right)[1 - \exp(-bt)];</math></p> <p>For progressive nucleation:  <math>\alpha \rightarrow \infty: I = \left(\frac{a}{t^{\frac{1}{2}}}\right)[1 - \exp(-Abt^2)]</math></p>
1987/M. Sluyters-Rehbach, J.H.O.J. Wijenberg, E. Bosco and J. H. Sluyters. [64]	Hemispherical infinite diffusion mass transfer model	<p>Group (3)</p> <p>Current transition function:  <math>I(t) = \frac{1}{\alpha(At)^{\frac{1}{2}}}(1 - \exp[-\alpha(At)^{\frac{1}{2}}\{(At)^{\frac{1}{2}} - e^{-At}\int_0^{(At)^{1/2}}e^{\lambda^2}d\lambda\}]</math></p>
1999/L. Heerman and A. Tarallo [65]	Hemispherical infinite diffusion mass transfer model	<p>Group (4)</p> <p>Current transition function:  <math>j(t) = zFDc(\pi Dt)^{\frac{1}{2}}\frac{\Theta}{\Theta}(1 - \exp[-\alpha N_0(\pi Dt)^{\frac{1}{2}}t^{\frac{1}{2}}\Theta]);</math></p> <p>For instantaneous nucleation: <math>\bar{\delta}(t) = (\pi Dt)^{\frac{1}{2}};</math></p> <p>For progressive nucleation: <math>\bar{\delta} = (3/4)(\pi Dt)^{\frac{1}{2}}</math></p>

**Table 1.** Cont.

Ref.	Theoretical Model	Current Transition Function Groups of Nucleation and Growth
1999/D'Ajello, P.C.T., Munford, M.L., Pasa, A. A [43]	Hemispherical finite diffusion mass transfer model	<p>Group (5)</p> <p>For instantaneous nucleation:</p> $j = 2\pi NDRzFc_0b \left( 1 + \frac{RN^{\frac{1}{2}}}{\sqrt{at}} \right) [1 - \exp(-at)];$ <p>For progressive nucleation:</p> $j = 2\pi N_{\infty} DRzFc_0b \left( 1 + \frac{\sqrt{2} R \sqrt{AN_{\infty}}}{\sqrt{a't}} \right) [1 - \exp(-a't^2)]$
2006/M.Y. Abyaneh [10]	Conical/hemispherical infinite diffusion mass transfer model	<p>Group (6)</p> <p>Conical model:</p> $(j)_{R.C.C.} = \frac{zF\rho}{M} \tan \alpha \frac{dR_0}{dt} [1 - \exp(-\pi R_0^2 N_0)];$ <p>Hemispherical model:</p> $(j)_{Hemi} = 2 \frac{zF\rho}{M} \frac{dR_0}{dt} \tau \exp(-\tau^2) \int_0^\tau \exp(s^2) ds$
2018/Vladimir A. Isaev, O.V., Grishenkova, Y.P. Zaykov [12]	Hemispherical multiple nucleation with kinetic controlled growth under linear diffusion mass transfer model	<p>Group (7)</p> <p>For instantaneous nucleation:</p> $j = 2 \frac{ze}{v} k_1 x \omega(x) = 2 \frac{ze}{v} k_1 x \exp(-x^2) \int_0^x \exp \xi^2 d\xi;$ <p>For progressive nucleation:</p> $j = 3 \frac{ze}{v} k_1 \omega_2(y) =$ $3 \frac{ze}{v} k_1 \exp(-y^3) \int_0^y (y^2 - \xi^2) \exp(3\xi^2 - 2\xi^3) d\xi$
2018/Luo, Gong, Li, Deyu, Yuan, Guohui and Li, Ning [14]	Cylindrical/hemispherical finite diffusion mass transfer mode	<p>Group (8)</p> <p>For instantaneous nucleation:</p> $I = zFc_0 D^{\frac{1}{2}} / \pi^{\frac{1}{2}} \left( \frac{\sqrt{\pi D}}{R} + \frac{1}{\sqrt{t}} \right) (1 - \exp(-N\pi kDt));$ <p>For progressive nucleation:</p> $I = zFc_0 D^{\frac{1}{2}} / \pi^{\frac{1}{2}} \left( \frac{\sqrt{\pi D}}{R} + \frac{1}{\sqrt{t}} \right) (1 - \exp(-AN_m \pi k'Dt^2 / 2))$

## 5. Conclusions

Nucleation and growth processes in electrochemical metal deposition determine the properties of the metal deposits. The study of nucleation and growth processes by electrochemical methods utilizing the current function of electrocrystallization to reveal the microcrystallization kinetic process has certain advantages over other methods of investigating heterogeneous nucleation. This brief review provides an updated state of the model, current transition of nucleation and growth during electrocrystallization, with some comments on their relative merits. Nucleation and growth processes play an important role in future electrochemical fabrication techniques, in particular, for the generation of nanoelectronic devices as well as for the development of new materials with unconventional properties. Furthermore, the shortcomings of the existing studies were pointed out, and improvement directions were proposed.

- (1) There has been no direct observation of the nucleation and growth process proposed by the theoretical model to the best of our knowledge. Thus, it is necessary to test the validity of the theoretical model using the experimental data obtained from the analysis of the actual nucleation and growth process on the electrode surface.
- (2) The transient current functions reported by various theoretical models are very complex and difficult to use. Some useful functions can be carried out to make the theoretical calculations and current measurements more convenient, and have great practical significance to the field of electrochemistry.
- (3) The correlation between the nucleation, growth, and microstructure of deposits has not been studied yet. That is, the correlation between the nucleation, growth, and microstructure of deposits is certainly desired to help gain deeper insights into the preparation of the microstructure in the future.

**Author Contributions:** (1) Substantial contributions to the conception and design, or acquisition of data, or analysis and interpretation of data: G.L., Y.Y., D.-Y.L., N.L., and G.-H.Y.; (2) Drafting the article or revising it critically for important intellectual content: G.L. and Y.Y.; (3) Final approval of the version to be published: G.L. and Y.Y.; (4) Agreement to be accountable for all aspects of the work in ensuring that questions related to the accuracy or integrity of any part of the work are appropriately investigated and resolved: G.L. and Y.Y. All authors have read and agreed to the published version of the manuscript.

**Funding:** This research was funded by the Research Project of Guangdong University of Petrochemical Technology (2019rc069); the Natural Science Project of Education Department of Guangdong Province (2021KTSCX079); the Science and Technology Project of Maoming City (2021019).

**Institutional Review Board Statement:** Not applicable.

**Informed Consent Statement:** Not applicable.

**Data Availability Statement:** Not applicable.

**Acknowledgments:** This study was performed with the support of the fund “Research Project of Guangdong University of Petrochemical Technology (2019rc069); the Natural Science Project of Education Department of Guangdong Province (2021KTSCX079); and the Science and Technology Project of Maoming City (2021019).

**Conflicts of Interest:** The authors declare no conflict of interest.

## Nomenclature

The following notations are for the essential parameters used in this work:

$I_m$	Peak value of current density ( $\text{mA}\cdot\text{cm}^{-2}$ )
$t_m$	The time value corresponding to the peak value of current density (s)
$I$	Current density of the whole electrode surface
$k$	$= (8\pi c/\rho)^{1/2}$ The numerical constant determined by the conditions of the experiment
$M$	Molecular weight of the deposited material ( $\text{g}\cdot\text{mol}^{-1}$ )
$\rho$	Density of the deposited material ( $\text{g}\cdot\text{cm}^{-3}$ )
$\rho/M$	Molar density of the species to be deposited ( $\text{mol}\cdot\text{cm}^{-3}$ )
$F$	Faraday constant ( $\text{C}\cdot\text{mol}^{-1}$ )
$z$	Number of electron transfer per ion
$zF$	Molar charge of the electrodepositing species
$t$	Electrodepositing time (s)
$c$	Bulk concentration ( $\text{mol}\cdot\text{cm}^{-3}$ )
$A$	Steady state nucleation rate constant per site ( $\text{s}^{-1}$ )
$D$	Diffusion coefficient ( $\text{cm}^2\cdot\text{s}^{-1}$ )
$e$	Elementary electric charge(C)
$v$	Volume of one atom of the deposit ( $\text{cm}^3$ )
$N$	Total number of nuclei [Group (1)]
$N_\infty$	Number density of active sites [Group (5)]
$K$	$= \frac{4}{3} \left( \frac{8\pi c M}{\rho} \right)^{\frac{1}{2}}$ , it is again evaluated by taking the limit $AN_\infty t \rightarrow 0$ and comparing it with $I(t) = \frac{2zFAN_\infty\pi(2Dc)^{3/2}M^{1/2}t^{3/2}}{3\rho^{1/2}}$
$N_0$	Number density of active sites at ( $\text{cm}^{-2}$ ) [Group (2)]
$a$	$= zFD^{1/2}c/\pi^{1/2} (A\cdot s^{1/2}\cdot\text{cm}^2)$ [Group (2)]
$b$	$= N_0\pi kD (\text{s}^{-1})$ [Group (2)]
$\alpha$	$= (2\pi)^{3/2}D(Mc/\rho)^{1/2}N_0/A$ [Group (3)]
$N_0$	Maximum number density of nuclei ( $\text{cm}^{-2}$ ) [Group (3)]
$\theta_{ex}$	Total coverage
$j(t)$	Total current density
$\bar{\delta}(t)$	Thickness of the diffusion layer
$\bar{\delta}$	Thickness of the uniform diffusion layer

$\emptyset$	$= 1 - \frac{e^{-At}}{(At)^{1/2}} \int_0^{(At)^{1/2}} e^{\lambda^2} d\lambda$
$\Theta$	$= 1 - (1 - e^{-At}) / At$
$\alpha$	$= 2\pi(2MDc/\rho)^{1/2}$ [Group (4)]
$N_0$	Rate of nucleation ( $\text{cm}^{-2}$ ) [Group (4)]
$R$	Critical distance for the interaction between the nucleus and Brownian motion region [Group (5)]
$b$	An appropriate proportional constant [Group (5)]
$a$	$= 4\pi ND$ [Group (5)]
$a'$	$= \frac{1}{2}AN_\infty 4\pi D$
$(j)_{\text{R.C.C.}} / (j)_{\text{Hemi}}$	Current density of conical nucleation model ( $\text{A}\cdot\text{cm}^{-2}$ )
$\alpha$	Angle of contact between nuclei and the substrate [Group (6)]
$R_0$	Radius of the base of a growth form (cm) [Group (6)]
$\tau$	$= R_0 \sqrt{\pi N_0}$
$s$	Area of the equi-concentration field of radius $r$ per unit area of the electrode surface
$k_1$	$= \text{const}$ , the rate nucleus growth ( $\text{cm}\cdot\text{s}^{-1}$ ) [Group (7)]
$x$	$= k_1(\pi n)^{1/2}t$
$n$	Number density of nuclei ( $\text{cm}^{-2}$ )
$r$	Hemispherical nucleus(cm) [Group (7)]
$\omega(x), \omega_2(y)$	Dawson's integral
$c_0$	Ion concentration under equilibrium conditions at time $t = 0$ [Group (8)]
$R$	Radius of finite diffusion mass transfer [Group (8)]

## References

- Budevski, E.; Staikov, G.; Lorenz, W. Electrocristallization: Nucleation and growth phenomena. *Electrochim. Acta* **2000**, *45*, 2559–2574. [[CrossRef](#)]
- Hyde, M.E.; Compton, R.G. A review of the analysis of multiple nucleation with diffusion controlled growth. *J. Electroanal. Chem.* **2003**, *549*, 1–12. [[CrossRef](#)]
- Grujicic, D.; Pesic, B. Electrodeposition of copper: The nucleation mechanisms. *Electrochim. Acta* **2002**, *47*, 2901–2912. [[CrossRef](#)]
- Milchev, A. Electrocristallization: Nucleation and growth of nano-clusters on solid surfaces. *Russ. J. Electrochim.* **2008**, *44*, 619–645. [[CrossRef](#)]
- Yan, C.; Jiang, L.L.; Yao, Y.X.; Lu, Y.; Huang, J.Q.; Zhang, Q. Nucleation and Growth Mechanism of Anion-Derived Solid Electrolyte Interphase in Rechargeable Batteries. *Angew. Chem. Int. Ed.* **2021**, *60*, 8521–8525. [[CrossRef](#)]
- Xu, J.; Ren, W.; Lian, Z.; Yu, P.; Yu, H. A review: Development of the maskless localized electrochemical deposition technology. *Int. J. Adv. Manuf. Technol.* **2020**, *110*, 1731–1757. [[CrossRef](#)]
- Macdonald, D.D. The history of the Point Defect Model for the passive state: A brief review of film growth aspects. *Electrochim. Acta* **2011**, *56*, 1761–1772. [[CrossRef](#)]
- Abyaneh, M.; Fleischmann, M.; Mehrabi, M. Modelling the growth of a single centre. *J. Electroanal. Chem.* **2019**, *834*, 114–123. [[CrossRef](#)]
- German, S.R.; Edwards, M.A.; Ren, H.; White, H.S. Critical nuclei size, rate, and activation energy of  $\text{H}_2$  gas nucleation. *J. Am. Chem. Soc.* **2018**, *140*, 4047–4053. [[CrossRef](#)]
- Abyaneh, M.Y. Modelling diffusion controlled electrocristallisation processes. *J. Electroanal. Chem.* **2006**, *586*, 196–203. [[CrossRef](#)]
- Isaev, V.A.; Zaykov, Y.P.; Grishenkova, O.V.; Kosov, A.V.; Semerikova, O.L. Analysis of Potentiostatic Current Transients for Multiple Nucleation with Diffusion and Kinetic Controlled Growth. *J. Electrochim. Soc.* **2019**, *166*, D851–D856. [[CrossRef](#)]
- Isaev, V.A.; Grishenkova, O.V.; Zaykov, Y.P. On the theory of 3D multiple nucleation with kinetic controlled growth. *J. Electroanal. Chem.* **2018**, *818*, 265–269. [[CrossRef](#)]
- Yuan, Y.; Luo, G.; Li, N. New in situ description of electrodepositing multiple nucleation processes under galvanostatic stimuli. *RSC Adv.* **2021**, *11*, 31526–31532. [[CrossRef](#)]
- Luo, G.; Li, D.; Yuan, G.; Li, N. Potentiostatic Current Transient for Multiple Nucleation: A Limited-Diffusion Process Description. *J. Electrochim. Soc.* **2018**, *165*, D147–D151. [[CrossRef](#)]
- Stranski, I.N. Zur theorie des kristallwachstums. *Z. Phys. Chem.* **2017**, *136*, 259–278. [[CrossRef](#)]
- Conway, B.; Bockris, J.O. On the calculation of potential energy profile diagrams for processes in electrolytic metal deposition. *Electrochim. Acta* **1961**, *3*, 340–366. [[CrossRef](#)]
- Fleischmann, M.; Thirsk, H. Anodic electrocristallization. *Electrochim. Acta* **1960**, *2*, 22–49. [[CrossRef](#)]
- Vermilyea, D. On the Theory of Electrolytic Crystal Growth. *J. Chem. Phys.* **1956**, *25*, 1254–1263. [[CrossRef](#)]
- Burton, W.-K.; Cabrera, N.; Frank, F. The growth of crystals and the equilibrium structure of their surfaces. *Philos. Trans. R. Soc. Lond. Ser. A Math. Phys. Sci.* **1951**, *243*, 299–358. [[CrossRef](#)]
- Seiter, H.; Fischer, H.; Albert, L. Elektrochemisch-morphologische studien zur erforschung des mechanismus der elektrokristallisation, fern vom anfangszustand. *Electrochim. Acta* **1960**, *2*, 97–120. [[CrossRef](#)]

21. Budevski, E. Some Fundamental Aspects of Electrocristallization. *Prog. Surf. Membr. Sci.* **1976**, *11*, 71–116.
22. Avrami, M. Kinetics of phase change. I General theory. *J. Chem. Phys.* **1939**, *7*, 1103–1112. [\[CrossRef\]](#)
23. Rangarajan, S. Electrocristallisation: Multilayer formation and potentiostatic transients. *J. Electroanal. Chem. Interfacial Electrochem.* **1973**, *46*, 125–129. [\[CrossRef\]](#)
24. Armstrong, R.; Fleischmann, M.; Thirsk, H. The anodic behaviour of mercury in hydroxide ion solutions. *J. Electroanal. Chem.* **1966**, *11*, 208–223. [\[CrossRef\]](#)
25. Bosco, E.; Rangarajan, S. Electrochemical phase formation (ECPF) and macrogrowth Part I. Hemispherical models. *J. Electroanal. Chem. Interfacial Electrochem.* **1982**, *134*, 213–224. [\[CrossRef\]](#)
26. Bosco, E.; Rangarajan, S. Electrochemical phase formation (ECPF) and macrogrowth Part II. Two-rate models. *J. Electroanal. Chem. Interfacial Electrochem.* **1982**, *134*, 225–241. [\[CrossRef\]](#)
27. Fleischmann, M.; Liler, M. The anodic oxidation of solutions of plumbous salts. Part 1-The kinetics of deposition of  $\alpha$ -lead dioxide from acetate solutions. *Trans. Faraday Soc.* **1958**, *54*, 1370–1381. [\[CrossRef\]](#)
28. Astley, D.J.; Harrison, J.A.; Thirsk, H.R. Electrocristallization of mercury, silver and palladium. *Trans. Faraday Soc.* **1968**, *64*, 192–201. [\[CrossRef\]](#)
29. Scharifker, B.R.; Mostany, J. Three-dimensional Nucleation with Diffusion Controlled Growth. *J. Electroanal. Chem.* **1984**, *177*, 13–23. [\[CrossRef\]](#)
30. Scharifker, B.; Hills, G. Theoretical and experimental studies of multiple nucleation. *Electrochim. Acta* **1983**, *28*, 879–889. [\[CrossRef\]](#)
31. Hills, G.; Schiffrian, D.; Thompson, J. Electrochemical nucleation from molten salts—I. Diffusion controlled electrodeposition of silver from alkali molten nitrates. *Electrochim. Acta* **1974**, *19*, 657–670. [\[CrossRef\]](#)
32. Hills, G.; Schiffrian, D.; Thompson, J. Electrochemical nucleation from molten salts—II: Time dependent phenomena in electrochemical nucleation. *Electrochim. Acta* **1974**, *19*, 671–680. [\[CrossRef\]](#)
33. Fanfoni, M.; Tomellini, M. The Johnson-Mehl-Avrami-Kohnogorov model: A brief review. *Il Nuovo Cim. D* **1998**, *20*, 1171–1182. [\[CrossRef\]](#)
34. Tomellini, M. Phase transformation kinetics of Voronoi cells in space tessellation governed by the Kolmogorov-Johnson-Mehl-Avrami model. *Phys. Lett. A* **2017**, *381*, 1067–1075. [\[CrossRef\]](#)
35. Alekseechkin, N.V. Extension of the Kolmogorov-Johnson-Mehl-Avrami theory to growth laws of diffusion type. *J. Non-Cryst. Solids* **2011**, *357*, 3159–3167. [\[CrossRef\]](#)
36. Farjas, J.; Roura, P. Cell size distribution in a random tessellation of space governed by the Kolmogorov-Johnson-Mehl-Avrami model: Grain size distribution in crystallization. *Phys. Rev. B* **2008**, *78*, 144101–144111. [\[CrossRef\]](#)
37. Ashworth, M.A.; Haspel, D.; Wu, L.; Wilcox, G.D.; Mortimer, R.J. An Investigation into the Effect of a Post-electroplating Electrochemical Oxidation Treatment on Tin Whisker Formation. *J. Electron. Mater.* **2014**, *44*, 442–456. [\[CrossRef\]](#)
38. Ren, X.; Song, Y.; Liu, A.; Zhang, J.; Yang, P.; Zhang, J.; An, M. Experimental and theoretical studies of DMH as a complexing agent for a cyanide-free gold electroplating electrolyte. *RSC Adv.* **2015**, *5*, 64997–65004. [\[CrossRef\]](#)
39. Ren, X.; Song, Y.; Liu, A.; Zhang, J.; Yang, P.; Zhang, J.; Yuan, G.; An, M.; Osgood, H.; Wu, G. Role of polyethyleneimine as an additive in cyanide-free electrolytes for gold electrodeposition. *RSC Adv.* **2015**, *5*, 64806–64813. [\[CrossRef\]](#)
40. Ren, X.; Song, Y.; Liu, A.; Zhang, J.; Yuan, G.; Yang, P.; Zhang, J.; An, M.; Matera, D.; Wu, G. Computational Chemistry and Electrochemical Studies of Adsorption Behavior of Organic Additives during Gold Deposition in Cyanide-free Electrolytes. *Electrochim. Acta* **2015**, *176*, 10–17. [\[CrossRef\]](#)
41. Zhang, J.; Liu, A.; Ren, X.; Zhang, J.; Yang, P.; An, M. Electrodeposit copper from alkaline cyanide-free baths containing 5,5'-dimethylhydantoin and citrate as complexing agents. *RSC Adv.* **2014**, *4*, 38012–38026. [\[CrossRef\]](#)
42. Kong, D.; Zheng, Z.; Meng, F.; Li, N.; Li, D. Electrochemical Nucleation and Growth of Cobalt from Methanesulfonic Acid Electrolyte. *J. Electrochem. Soc.* **2018**, *165*, D783–D789. [\[CrossRef\]](#)
43. D'Ajello, P.C.T.; Munford, M.L.; Pasa, A.A. Transient equations for multiple nucleation on solid electrodes: A stochastic description. *J. Chem. Phys.* **1999**, *111*, 4267–4272. [\[CrossRef\]](#)
44. Palomar-Pardavé, M.; Scharifker, B.R.; Arce, E.M.; Romero-Romo, M. Nucleation and diffusion-controlled growth of electroactive centers: Reduction of protons during cobalt electrodeposition. *Electrochim. Acta* **2005**, *50*, 4736–4745. [\[CrossRef\]](#)
45. D'Ajello, P.C.T.; Fiori, M.A.; Pasa, A.A.; Kipervaser, Z.G. Reaction-Diffusion Interplay in Electrochemical Deposition Processes A Theoretical Approach. *J. Electrochem. Soc.* **2000**, *147*, 4562–4566. [\[CrossRef\]](#)
46. Luo, G.; Yuan, G.; Li, N. Cyanide-free Electrolyte for Au (III) and Au (I) Electrodepositing Using DMH as Complexing Agent. *RSC Adv.* **2016**, *6*, 61341–61345. [\[CrossRef\]](#)
47. Sebastián, P.; Botello, L.E.; Vallés, E.; Gómez, E.; Palomar-Pardavé, M.; Scharifker, B.R.; Mostany, J. Three-dimensional nucleation with diffusion controlled growth: A comparative study of electrochemical phase formation from aqueous and deep eutectic solvents. *J. Electroanal. Chem.* **2016**, *793*, 119–125. [\[CrossRef\]](#)
48. Glioza, A.S.; Alexe-Ionescu, A.L.; Barbero, G. Ohmic model for electrodeposition of metallic ions. *Phys. Lett. A* **2015**, *379*, 2657–2660. [\[CrossRef\]](#)
49. Ustarroz, J.; Ke, X.; Hubin, A.; Bals, S.; Terryn, H. New Insights into the Early Stages of Nanoparticle Electrodeposition. *J. Phys. Chem. C* **2012**, *116*, 2322–2329. [\[CrossRef\]](#)
50. Heerman, L.; Tarallo, A. Electrochemical nucleation with diffusion-limited growth. Properties and analysis of transients. *Electrochim. Commun.* **2000**, *2*, 85–89. [\[CrossRef\]](#)

51. Altimari, P.; Greco, F.; Pagnanelli, F. Nucleation and growth of metal nanoparticles on a planar electrode: A new model based on iso-nucleation-time classes of particles. *Electrochim. Acta* **2019**, *296*, 82–93. [[CrossRef](#)]
52. D’Ajello, P.C.T.; Pasa, A.A.; Munford, M.L.; Schervenski, A.Q. The effects of temperature on current–potential profiles from electrochemical film production: A theoretical approach. *Electrochim. Acta* **2008**, *53*, 3156–3165. [[CrossRef](#)]
53. D’Ajello, P.C. Current–time and current–potential profiles in electrochemical film production. (I) Current–time curves. *J. Electroanal. Chem.* **2004**, *573*, 29–35. [[CrossRef](#)]
54. Hyde, M.E.; Compton, R.G. Theoretical and experimental aspects of electrodeposition under hydrodynamic conditions. *J. Electroanal. Chem.* **2005**, *581*, 224–230. [[CrossRef](#)]
55. Stephens, R.M.; Willis, M.; Alkire, R.C. Additive-Assisted Nucleation and Growth by Electrodeposition. *J. Electrochem. Soc.* **2009**, *156*, D385–D394. [[CrossRef](#)]
56. Branco, P.D.; Mostany, J.; Borrás, C.; Scharifker, B.R. The current transient for nucleation and diffusion-controlled growth of spherical caps. *J. Solid State Electrochem.* **2008**, *13*, 565–571. [[CrossRef](#)]
57. Mazaira, D.; Borrás, C.; Mostany, J.; Scharifker, B.R. Three-dimensional nucleation with diffusion-controlled growth: Simulation of hierarchical diffusion zones overlap. *J. Electroanal. Chem.* **2009**, *631*, 22–28. [[CrossRef](#)]
58. Mamme, M.H.; Deconinck, J.; Ustarroz, J. Transition between kinetic and diffusion control during the initial stages of electrochemical growth using numerical modelling. *Electrochim. Acta* **2017**, *258*, 662–668. [[CrossRef](#)]
59. Guo, L.; Searson, P.C. Simulations of Island Growth and Island Spatial Distribution during Electrodeposition. *Electrochim. Solid-State Lett.* **2007**, *10*, D76–D78. [[CrossRef](#)]
60. Guo, L.; Searson, P.C. On the influence of the nucleation overpotential on island growth in electrodeposition. *Electrochim. Acta* **2010**, *55*, 4086–4091. [[CrossRef](#)]
61. Guo, L.; Oskam, G.; Radisic, A.; Hoffmann, P.M.; Searson, P.C. Island growth in electrodeposition. *J. Phys. D Appl. Phys.* **2011**, *44*, 443001–443012. [[CrossRef](#)]
62. Ustarroz, J.; Hammons, J.A.; Altantzis, T.; Hubin, A.; Bals, S.; Terryn, H. A generalized electrochemical aggregative growth mechanism. *J. Am. Chem. Soc.* **2013**, *135*, 11550–11561. [[CrossRef](#)]
63. Velmurugan, J.; Noël, J.-M.; Nogala, W.; Mirkin, M.V. Nucleation and growth of metal on nanoelectrodes. *Chem. Sci.* **2012**, *3*, 3307–3314. [[CrossRef](#)]
64. Sluyters-Rehbach, M.; Wijenberg, J.H.O.J.; Bosco, E.; Sluyters, J.H. The Theory of Chronoamperometry for the Investigation of Electrococrystallization. *J. Electroanal. Chem.* **1987**, *236*, 1–20. [[CrossRef](#)]
65. Heerman, L.; Tarallo, A. Theory of the chronoamperometric transient for electrochemical nucleation with diffusion-controlled growth. *J. Electroanal. Chem.* **1999**, *470*, 70–76. [[CrossRef](#)]